

**Effect of High Temperature Steam Oxidation on Yielding of Zircaloy-4
PWR Fuel Cladding
-Expanding Copper Mandrel Test-**

Kye-Ho Nho and Sun-Pil Choi
Korea Advanced Energy Research Institute

Byong-Whi Lee
Korea Advanced Institute of Science and Technology
(Received March 24, 1989)

**가압경수형 핵연료 피복관 지르칼로이-4의 항복현상에 대한 고온
수증기 산화의 영향
-구리 맨드렐 팽창시험법-**

노계호 · 최순필
한국에너지연구소

이 병 휘
한국과학기술원
(1989. 3. 24 접수)

Abstract

With the Zircaloy-4 tube oxidized in high temperature (1323 K) steam for 5, 10, 30 and 60 minutes, the expanding copper mandrel test was carried out over a temperature range of 673-1173K at $\dot{\epsilon} = 3.0 \times 10^{-5} \text{ S}^{-1}$. The oxidation parameters (K_i) in the present study were linearly proportional to square root of time ($K_i = \delta \sqrt{t}$) and their rate constants (δ) are 0.281, 2.82, and 2.313 for weight gain and thickness of ZrO₂ and α (O) layer, respectively.

Activation energy for high temperature (873-1073K) plastic deformation of Zircaloy-4 increases from 251 KJ/mol to 323 KJ/mol with increase in oxidation time from 5 minutes to 60 minutes due to the high strengthened ZrO₂. With the oxide layer thickness [K_i ; expressed in "Equivalent Cladding Reacted"(ECR, %)] and the yield stress obtained from the mandrel test, an empirical relation was derived as $(\sigma/C)^n = K \exp(-Q/RT)$ with $n=6.9$, $m=5.7$, $C=0.155, 0.138, 0.051, \text{ and } 0.046 \text{ MPa}$ for $Q=251, 258, 316, 323 \text{ KJ/mol}$, respectively.

요 약

고온 수증기(1323 K) 분위기에서 산화시킨 지르칼로이-4 피복관으로, 구리 맨드렐 팽창 시험(Copper Mandrel Expansion Test)을 변형률(Strain Rate)이 $3.0 \times 10^{-5} / \text{sec}$ 일때 673-

1173 K 온도 범위에서 수행하였다. 본 연구에서, 산화매개변수(Ki)는 시간(t)의 제곱근에 비례하고($K_i = \delta_{\text{ki}} t^{\frac{1}{2}}$), 비례상수(δ_{ki})는 무게증가(Weight Gain), ZrO₂의 두께, $\alpha(0)$ 층에 대하여 각각 0.281, 2.82, 2.313을 사용하였다. 지르칼로이-4의 고온(873-1073 K) 소성변형에 의한 활성화 에너지는 ZrO₂가 높은 강도를 갖기 때문에 산화 시간이 5분에서 60분으로 증가함에 따라 251 KJ/mol에서 323 KJ/mol로 증가하였다. 산화막 두께, K와 항복 응력의 관계는 $(\sigma/C)^n = K^m \exp(Q/RT)$ 인 관계식을 얻었다. 여기서 n은 6.9, m은 5.7, 그리고 Q가 251, 258, 316, 323KJ/mol에 대해 C는 0.155, 0.138, 0.051, 0.046MPa이다.

1. Introduction

Since zirconium-based alloys generally have a low thermal neutron cross-section and good high temperature mechanical and corrosion resistance properties,¹⁾ much study has been continued to develop proper materials for pressure tube and cladding material on thermal neutron nuclear reactor system. Zircaloy-4, which is now commonly used as cladding material of nuclear fuel, is one of them.

Under the conditions of a loss-of-coolant accident in a watercooled reactor, the cladding temperature will be elevated in a steam atmosphere. During this period, an oxide film on the cladding surface and gradient of oxygen concentration into the cladding matrix are formed by reaction of Zircaloy with high temperature steam.²⁾

As time goes, the oxide film develop to thicker oxide layer. Such a formation of oxide layer causes embrittlement and increases the probability of failure of cladding materials when certain conditions are reached.³⁾

In the current acceptance criteria³⁾ for an emergency core cooling system (ECCS) in the licensing of light water reactors, the steam oxidation of the cladding is limited to not more than 17%(permissible equivalent cladding reacted, ECR) of the wall thickness in order to avoid severe embrittlement of the oxidized cladding.

Increase in applied hoop stress, which produces a specified amount of yield, due to increase in the thickness of oxide layer has very important rela-

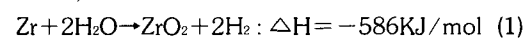
tion with failure of cladding tube.

Thus, the purpose of the present study is to obtain an empirical relation between applied hoop stress and thickness of oxide layer (expressed in ECR, %) through expanding copper mandrel test.^{4,5)}

2. Theory

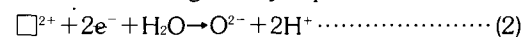
2.1 Oxidation

Steam oxidation is primarily a reaction of the outer surface of the fuel rod cladding. Under accident conditions, simultaneous oxidation of the inner cladding tube surface can take place caused by cladding rupture and steam inward diffusion. Steam oxidation appears, according to the reaction,¹⁾

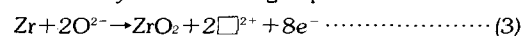


However, the basic mechanism is much more complex. At temperatures above the $\alpha - \beta$ transition, the oxidation of Zircaloy involves the formation of layers of oxide (nominally ZrO₂) and oxygen stabilized alpha ($\alpha(0)$). The growth of the oxide and alpha layer into the beta region is governed by diffusion processes,⁶⁾ that is, diffusion of oxygen ions and anionic vacancies (represented by the symbol \square^{2+}).

The reaction at the interface between steam and the oxide can be given by equation.⁷⁾



These oxygen ions diffuse in and react with the $\alpha(0)$ to form oxide, electrons and anionic vacancies as shown by the following equation⁷⁾:



These electrons and anionic vacancies diffuse out to continue the corrosion process. It is to be noted that for zirconium the oxidation proceeds by the diffusion of oxygen ions into the oxide and not by diffusion of the metal out through the oxide.⁸⁾ The basic kinetic parameters for oxide growth, alpha layer growth and weight gain can be reasonably well described by parabolic kinetics represented by equations of the form:⁶⁾

$$\frac{dK_i}{dt} = \frac{\delta^2 K_i}{2K_i} \dots\dots\dots (4)$$

where K_i =kinetic parameter (oxide layer thickness, μ m, and weight gain, mg/cm²) t =time, sec., $\delta^2 K_i$ =rate constant for K_i .

For ideal isothermal behavior($K_i=0$ at $t=0$)

$$K_i = \delta^2 K_i t \dots\dots\dots (5)$$

At least at oxidation temperature above about 1273 K, oxide layer appear to be represented satisfactorily in the early stages by the simple parabolic kinetics noted in Eqs. (4) and (5).

2.2 Mandrel Test

As the power increases rapidly, the different thermal expansion coefficient between uranium-dioxide and Zircaloy cladding causes them to contact. If internal pressure which is induced by contact is greater than yield stress of Zircaloy cladding,

the cladding deform plastically. And if there is a defect or region with high stress concentration which is induced mechanically or chemically, the cladding will fail abruptly.

The expanding mandrel test has been used as a laboratory technique for simulating fuel rod pellet-cladding-interaction(PCI)^{9,10)}

Large difference of thermal expansion coefficient value between copper as expanding mandrel and Zircaloy-4 cladding is sufficient to simulate contact pressure between pellet and cladding. But copper mandrel test has two limitations. First, the temperature limitation, that is, the temperature below 673 K is not applicable because induced plastic deformation of oxidized Zircaloy-4 cladding tube is too small to detect. Strengthening due to oxidation makes the plastic deformation more difficult. Secondly, the strain-rate limitation, that is, the strain-rate above 10⁻⁴ s⁻¹ can not be obtained with high frequency induction heating rate used in the present experiment. Thus, this test can not be used to cause cladding rupture.

2.2.1 Yield Pressure of Oxidized Zircaloy Tube

The yield pressure of oxidized Zircaloy tube is given as follows^{4,5)};

$$P = \frac{d + (\alpha_{1a} - \alpha_{2b}) \cdot \Delta T - \bar{d}_p^0 (1 + \alpha_{22} \Delta T) + t_0 \left(\frac{b'}{b' + d_e' + p_e'} - 1 \right)}{\frac{a'}{E_1} \cdot (1 - \nu_1) + \frac{2b'^2 c'}{E_2 \cdot (c'^2 - b'^2)}} \dots\dots\dots (6)$$

where

- p : Contact pressure of Zircaloy tube at yield point
- a : Initial mandrel radius at room temperature
- b : Initial (oxidized) Zircaloy inner radius at room temperature
- a' : Changed mandrel radius by thermal expansion at temperature T_0
- b' : Changed Zircaloy inner radius by thermal expansion at temperature T_0
- c' : Changed Zircaloy outer radius by thermal ex-

- pansion at temperature T_0
- d : Initial clearance between mandrel outer radius and Zircaloy inner radius at room temperature
- d_e' : The expansion or contraction of Zircaloy inner radius by elastic deformation at temperature T_0
- d_p' : The expansion of Zircaloy inner radius by plastic deformation at temperature T_0
- d_p^0 : The plastic expansion of Zircaloy outer radius after cooling to room temperature
- E_1 : Young's modulus of copper mandrel

E_z : Young's modulus of oxidized Zircaloy-4 clad

ΔT : $T_{test} - T_{room}$

t_0 : Thickness of Zircaloy clad at test temperature

α_1 : Thermal expansion coefficient of copper mandrel at the reference temperature of 298 K

α_2 : Thermal expansion coefficient of oxidized Zircaloy clad at the reference temperature of 308 K

ν_1 : Poisson's ratio of copper mandrel

Since E_z and α_2 in Eq.(6) are the Young's modulus and the thermal expansion coefficient of the oxidized Zircaloy tube, respectively, they are calculated as,⁽¹⁾

$$E_z = E^I T^I + E^{II} T^{II} \dots \dots \dots (7)$$

$$\alpha_2 = \frac{d^I K^I F^I / \rho^I + d^{II} K^{II} F^{II} / \rho^{II}}{K^I F^I / \rho^I + K^{II} F^{II} / \rho^{II}} \dots \dots \dots (8)$$

where, superscripts I and II: ZrO₂ and α -Zr or oxidized Zircaloy tube, respectively.

T: fractional thickness

K: bulk modulus

F: fractional weight

ρ : density

2.2.2 Stress of Oxidized Zircaloy Tube

By thin wall approximation, the hoop stress, α_θ , of Zircaloy tube is:

$$\alpha_\theta = \frac{P \cdot (b' + d_p)}{t_0 + \Delta t} \dots \dots \dots (9)$$

where, Δt =change of Zircaloy clad thickness by contact pressure at test temperature

The radial stress, α_r , of Zircaloy tube is:

$$\alpha_r = -\frac{P}{2} \dots \dots \dots (10)$$

where outer pressure of Zircaloy tube is negligible in a vacuum. Since there is no axial deformation, there is no axial load. That is,

$$\alpha_z = 0 \dots \dots \dots (11)$$

To convert biaxial stresses to the effective stress,

$$\sigma_{eff} = \frac{1}{\sqrt{2}} [(\sigma_r - \sigma_\theta)^2 + (\sigma_\theta - \sigma_z)^2 + (\sigma_z - \sigma_r)^2] \dots \dots \dots (12)$$

Substituting Eq.(9), E.(10), and Eq.(11) into Eq.(12), the result is given by:

$$\begin{aligned} \sigma_{eff} &= \frac{1}{\sqrt{2}} [(\sigma_\theta)^2 + \sigma_r^2 + (\sigma_\theta - \sigma_r)^2]^{1/2} \\ &= \frac{1}{\sqrt{2}} \left[\left\{ \frac{P(b' + d_p)}{t_0 + \Delta t} \right\}^2 + \left\{ \frac{P + 0.1013}{2} \right\}^2 \right. \\ &\quad \left. + \left\{ \frac{P(b' + d_p)}{t_0 + \Delta t} + \left(\frac{P + 0.1013}{2} \right) \right\}^2 \right] \dots \dots \dots (13) \end{aligned}$$

This σ_{eff} may be equal to σ_y by maximum shear strain energy theory(Von-Mises' yield criterion).^(12,13)

2.3 Mechanical Properties of Composite Material

As it is almost impossible to measure the mechanical properties of the individual components of oxidized composite, it is essential to conduct tensile test on the composite, that is, direct measurement of effective yield strength and effective Young's modulus of composite to interpret its mechanical properties. Oxidized Zircaloy-4 in this experiment is a laminated composite reinforced by strong second phase of two-dimensional shapes⁽⁴⁾. The fractions of oxide layer (ZrO₂) and matrix are obtained from "Equivalent Cladding Reacted (ECR, %)" calculated by weight gain during oxidation.⁽³⁾ Mechanical properties of composite related with present work are described as follows.

2.3.1 Young's Modulus and Thermal Expansion Coefficient

Young's modulus (E) is generally dependent upon temperature and is a unique mechanical property of a material. The situation is obviously similar to that for the thermal expansion coefficient (α). At a moderate temperature, thermal expansion coefficient is inversely proportional to the square of Young's modulus⁽⁵⁾, that is,

$$\alpha(T) \propto \frac{1}{E^2(T)} \dots \dots \dots (14)$$

Crystals with low thermal expansion coefficients often have high Young's modulus. In laminar sys-

tem, the overall modulus is intermediate between the high-and the low-modulus components.

For the case of present system, the total applied stress (σ) on the cross-sectional area (A) of cladding is, by definition,

$$\sigma = \frac{F}{A} \dots \dots \dots (15)$$

where $F = \sum_i F_i$: sum of forces applied on cross-section of each component i

since $F_i = A_i \sigma_i$ and $\sigma_i = E_i \epsilon_i$,

$$\sigma = \sum_i \frac{A_i}{A} E_i \epsilon_i$$

Again since $\epsilon_i = \epsilon$, that is, the strain (ϵ) is the same magnitude for all components,

The effective Young's modulus, E_{eff} , is then given by

$$E_{eff} = \frac{\sigma}{\epsilon} = \sum_i \frac{A_i}{A} E_i$$

For the two lamina system,

$$E_{eff} = \frac{A_1}{A} E_1 + \frac{A_2}{A} E_2 = \frac{A_1}{A} E_1 + (1 - \frac{A_1}{A}) E_2 \dots \dots (16)$$

where $\frac{A_i}{A}$ is the fractional area of component i . This is the rule-of-mixture known as the first (Voigt) model.¹¹⁾

Thermal expansion coefficient for the composite can be calculated if we assume that no cracks develop, the contraction of each component is the same as the overall contraction, and all microstructures are pure hydrostatic (interfacial shear is negligible). Then the stress on each component is given by¹¹⁾

$$\sigma_i = K(\alpha_r - \alpha_i) \Delta T \dots \dots \dots (17)$$

where α_r and α_i are the average and individual volume expansion coefficient of a composite, ΔT is the temperature change from the stress-free state, and K is the bulk modulus, ($K = -P/(\Delta V/V) = E/3(1-2\nu)$), where P is the hydrostatic pressure, V the volume, E the elastic modulus, and ν Poisson's ratio). If the stress is nowhere large enough to disrupt the structure, the summation of stresses over the whole area is zero. Consequently, if the V_1 and V_2 are the fractional volumes for

composite,

$$K_1(\alpha_r - \alpha_1)V_1 \Delta T + K_2(\alpha_r - \alpha_2)V_2 \Delta T + \dots \dots = 0 \quad (18)$$

$$V_i = \frac{F_i \rho_r}{\rho_i}$$

Where F_i is the weight fraction of component i , and ρ_r and ρ_i are the mean and individual densities of a composite. Substituting Eq.(19) in Eq.(18) and eliminating ΔT , and ρ_r , an expression for the coefficient of volume expansion of the composite is the same as Eq.(8), that is

$$\alpha_r = \frac{\alpha_1 K_1 F_1 / \rho_1 + \alpha_2 K_2 F_2 / \rho_2 + \dots \dots}{K_1 F_1 / \rho_1 + K_2 F_2 / \rho_2 + \dots \dots}$$

2.3.2 Yield Strength and Plasticity

Yielding under uniaxial tension can occur in the components where the stress exceeds their yield strength. As an average, it is convenient to consider a so-called "critical yield strain criterion".¹⁴⁾ For a component of the yield strength (σ_{y_i}) and Young's modulus (E_i), the strain for yielding is

$$\epsilon_{y_i} = \sigma_{y_i} / E_i \dots \dots \dots (20)$$

A criterion for the yield of a composite will be decided by this experimental condition ;

$$\epsilon_{yc} > \epsilon_{y_1}, \epsilon_{y_2}, \dots \dots \epsilon_{y_n} \dots \dots \dots (21)$$

where ϵ_{yc} is called as the critical yield strain. This criteria can be re-written in terms of stress as,

$$\sigma_{yc} / E_c > \sigma_{y_1} / E_1, \sigma_{y_2} / E_2, \dots \dots, \sigma_{y_n} / E_n \quad (22)$$

The predicted yield strength of such a composite is thus given by

$$\sigma_{yc} = \sigma_{y^*} E_c / E^* = (\sigma_{y^*} / E^*) (E_1 V_1 + E_2 V_2 + \dots + E_n V_n) \dots \dots \dots (23)$$

where σ_{y^*} and E^* are the yield strength and Young's modulus of the component lamina having the highest σ_y/E_c ratio, and V_1, V_2, \dots, V_n are the volume fractions of the individual component of a composite. Thus, Young's modulus of a composite can be obtained from the summation of multiplication the individual modulus of each component by their fractional volume or area or thickness according to the type of a composite.

3. Experiment

3.1 Speciment Preparation

The Zircaloy-4 tube specimens used in this experiment have average dimension of 25mm length with 10.744mm outer diameter and 0.629mm wall thickness and were supplied by Sandvik, Sweden.

All the specimens are cleaned in a ultrasonic cleaner with alcohol and acetone. After cleaning, many of them are oxidized and some are heat-treated in a vacuum to use as control specimens.

Copper mandrel is commercially provided 99% copper rod and it is machined 40mm length and various diameter size to 0.005mm accuracy to give various initial clearance. The chemical composition

of Zircaloy-4 cladding and mechanical properties of the cladding, ZrO₂,^{16,17,18)} and copper mandrel¹⁹⁾ are presented in table 1 and Table 2, respectively.

Table 1. Chemical Composition of Zircaloy-4 Cladding

Alloying Elements	Contents
Tin	1.20–1.70 wt%
Iron	0.18–0.24 wt%
Chromium	0.07–0.13 wt%
Tot. Fe+Cr	0.28–0.37 wt%
Carbon	80–300 ppm
Oxygen	900–1400 ppm
Zr+Impurities	Balance

Table 2. Mechanical Properties of Zircaloy-4, ZrO₂, and Copper

Material Property	Zircaloy-4	ZrO ₂	Copper
Thermal Expansion coeff. (α , 1/K)	$(6.72 \times 10^{-6}T - 2.07 \times 10^{-3})/T - 308$	7×10^{-6}	$[0.3 + 2.167 \times 10^{-3}(T - 500)] / 100(T - 298)$
Young's Modulus (E, MPa)	$[9.9 \times 10^3 - 5.669(T - 273)] \times 9.81$	$[138 - 0.024(T - 273)] \times 10^3$	i) $T/T_m < 0.5$: $[117.24 - 21(T/T_m - 0.22)] \times 10^3$ ii) $T/T_m < 0.5$: $[111.4 - 21(T/T_m - 0.5)] \times 10$
Poisson's Ratio (ν)	$0.3303 + 8.376 \times 10^{-5}(T - 273)$	0.30	0.33
Density (ρ , gr/cm ³)	6.6	5.80	8.94

3.2 Apparatus

3.2.1 Oxidation and Heat-Treatment

Steam is produced by heating the distilled water in a flask and introduced into a quartz tube which has been externally heated by a resistance furnace. Control specimens are heat-treated in the induction furnace with a vacuum of 5×10^{-5} TORR.

3.2.2 Mandrel Test

The specimen set is composed of copper mandrel, Zircaloy-4 tube and temperature measurement equipment. Temperature of specimen is measured with chromel-alumel type thermocouple. To ensure a tight contact between the copper mandrel and the inner wall of Zircaloy tube, liquid nitrogen is used for reducing the mandrel diameter.

The specimens are heated to test temperatures

in an induction furnace with a vacuum of 5×10^{-5} TORR. The test apparatus is shown in Fig.1.

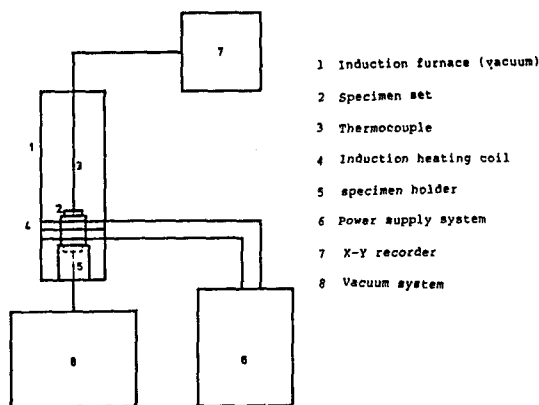
Strain rate is controlled by varying the heating rate. Increase in inner and outer diameter are measured with cylinder gauge and micrometer, respectively.

3.3. Experimental Test

3.3.1 Oxidation and Heat-Treatment

Oxidation is performed at high temperature (1323 K) steam for 5, 10, 30 and 60 minutes. The amount of oxidation is obtained by measuring the weight gain, and the thickness of ZrO₂ layer and of oxygen stabilized α -phase are measured by a metallographic observation. The result of oxidation in terms of temperature and time is presented in Table 3 and oxidation parameters such as weight

gain together with ECR and oxide layer thickness are plotted with respect to oxidation time as shown in Fig.2 and Fig.3 respectively.



* This apparatus was also used for heat-treatment of control specimen.

Fig.1 Schematic Diagram of Mandrel Test System

Table 3. Experimental Results of Oxidation as a Function of Oxidation time at 1323 K

Oxid. Time (min)	Oxidation induced strain (t-to/to)	Wt. gain (mg/cm ²)	Thickness (μ m)			Ratio of oxide layer to ini. clad th's (%)	Oxygen conc.		Equivalent cladding Reacted(ECR,%) by	
			ZrO ₂	α (o)	core		wt. %	at. %	H _k	wt. gain
5	0.06106	4.074	41.5	35	592.5	12.13	2.03	10.57	12.0	7.9
10	0.07538	7.718	83.5	41	546	19.97	3.78	18.30	16.7	15.6
30	0.12177	11.647	119.5	96	480	34.76	5.63	25.38	29.3	22.9
60	0.18569	16.190	161.5	152.5	401.5	50.48	7.63	32.02	38.3	31.0

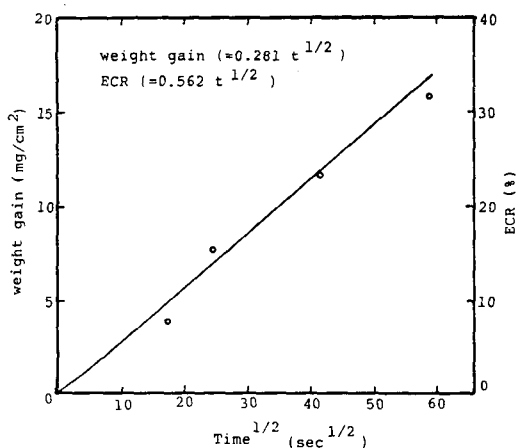


Fig.2 Variation of Weight Gain and Equivalent Cladding Reacted(ECR) with Oxidation Time

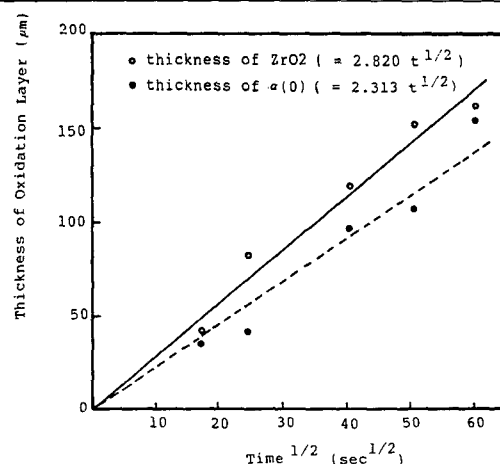


Fig.3 Variation of Thickness of Oxidation Layer with Oxidation Time

3.2.2 Mandrel Test

Since uniaxial tensile test of the oxidized composite tube is practically difficult to perform, expanding copper mandrel test is applied to obtain the yield stress. The range of test temperature is from 673 K to 1173 K with interval of 50K.

Firstly, ID and OD of specimens and diameter of copper mandrel rod are measured and then put assembled specimen set into an induction furnace with a vacuum of 5×10^{-5} TORR. When test temperature is reached, it is furnace-cooled to room temperature and then increase in ID and OD are measured. With the test data and mechanical properties of oxidized composite, yield stress is calculated from the analytical method,^{4,5)} and the results are shown in Fig.4 and Fig.5.

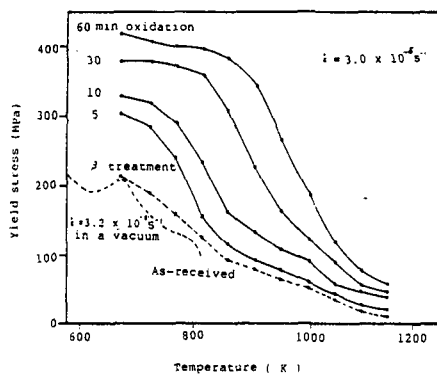


Fig.4 Temperature Dependence of Yield Stress at Various Oxidation Conditions

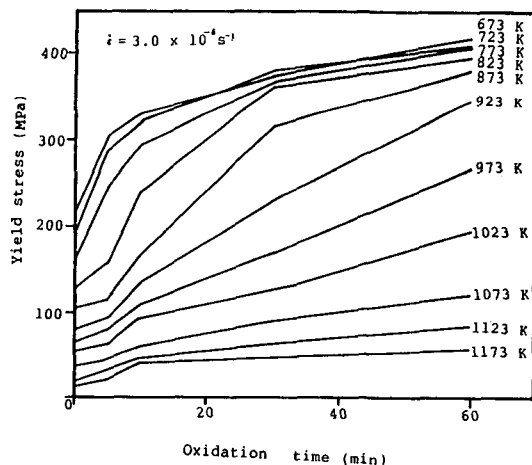


Fig.5 Oxidation Time Dependence of Yield Stress at Various Temperatures

4. Results and Discussion

4.1 Characteristics of Oxidized Zircaloy Tube

4.1.1 Microstructure

Exposure to a high temperature (1323K) steam environment causes change in the microstructure of the Zircaloy tube due to diffusion of oxygen into the matrix. This structure of the exposed material consists of layers of ZrO₂, oxygen-stabilized α -Zr, and a Widmanstätten β transformed phase as shown clearly in Fig.6(a)-(b). It is also shown that grain growth occurs as oxidation time increases.

α -Zirconium has the hexagonal close-packed structure below 1103K, and zirconium alloys exhibit anisotropic mechanical properties in different direction. This is because only few deformation systems operate in the hexagonal crystal structure of α -zirconium.²⁰⁾

4.1.2 Kinetics of Oxidation

A relationship between oxidation (kinetic) parameter and time for the present work can be expressed as Eq.(5)

$$, \text{ or } K_i = \delta \cdot kt^{\frac{1}{2}}$$

Values of rate constant for K_i ($\delta \cdot kt^{\frac{1}{2}}$) are obtained by linear regression fitting of data.²¹⁾ Fig.2 shows a plot in terms of weight gain and ECR vs. square root of time ($t^{\frac{1}{2}}$), simultaneously and their relations are $K_1 = 0.281t^{\frac{1}{2}}$ and $K_2 = 0.562t^{\frac{1}{2}}$, respectively. 17% of ECR as a ECCS criteria³⁾ can be obtained after oxidation at 1323K for about 12.5min. and is equivalent with total oxide layer thickness of 155 μ m and 8.5 mg/cm² wt. gain.

Also, thickness of ZrO₂ and $\alpha(0)$ are plotted with respect to $t^{\frac{1}{2}}$ in Fig.3 with relations of $K_3 = 2.82t^{\frac{1}{2}}$, $K_4 = 2.313t^{\frac{1}{2}}$, respectively.

From these results, oxidation parameter (K) is linearly proportional to square root of time very well.

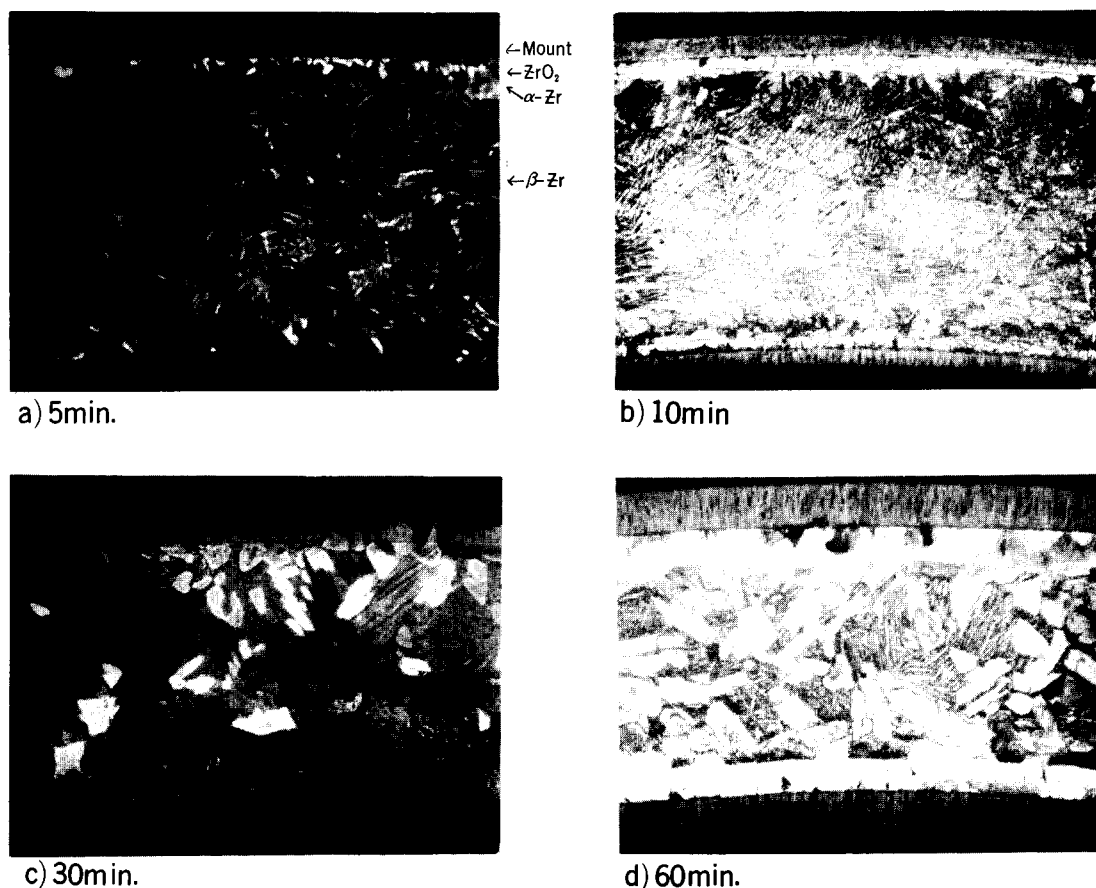


Fig.6 Microstructure of Zircaloy-4/Oxide Composite Specimen Oxidized at 1323K×1000

4.2 Yield Stress of Oxidized Zircaloy Tube

From the Fig.4 and Fig.5, it is to be noted that yield stress is increased as oxidation time is longer due to the increase in thickness of high strengthened ZrO₂, however, the extent of increase is larger at lower temperature than at higher one.

At high temperature of all oxidation conditions, recovery on the cold-worked state makes strain-hardened material ductile, and lowers the yield stress. Also increase in grain size(D) and/or decrease in dislocation density(ρ) at high temperature in Hall-Petch Eq.¹⁶⁾

that is,

$$\begin{aligned} \sigma_y &= \sigma_i + k^1 D^{-1/2} \\ &= \sigma_i + k^1 \rho^{1/2} \dots \dots \dots (24) \end{aligned}$$

where σ_y : yield stress
 σ_i : friction stress
 k^1 : unpinning constant
 D : grain diameter
 ρ : dislocation density
 decrease the yield stress

4.3 Activation Energy for Plastic Deformation of Oxidized Zircaloy Tube

If the plastic deformation of Zircaloy-4 is thermally activated, the activation energy can be obtained by following procedures. Strain rate can be represented by Arrhenius type equation,²²⁾ as follows

$$\dot{\epsilon} = A \sigma^n \exp(-Q/RT)$$

, or $\sigma^n = \dot{\epsilon} / A \exp(Q/RT)$ (25)
 Taking common logarithms on both sides of Eq.(25) :

$$\log \sigma = \frac{1}{n} \log(\dot{\epsilon} / A) + \frac{Q}{2.3nR} \frac{1}{T} \dots\dots\dots (26)$$

where Q is the activation energy for plastic deformation and R is the gas constant (8.314J/mole K). Plotting the data in terms of log σ vs. 1/T, the data show almost straight lines in the temperature range 873–1073 K as shown in Fig.7 with the various slopes.

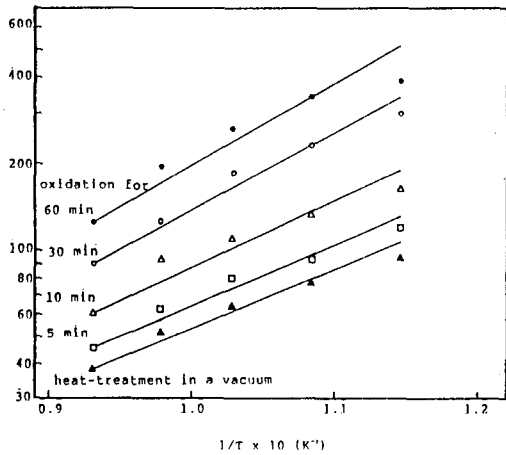


Fig.7 Variation of Yield Stress with Temperature at Various Oxidation conditions

From Eq.(26), slope = $\frac{Q}{2.3nR}$

Therefore, activation energy, Q, is given by :

$$Q = 2.3nr \cdot \text{slope}$$

Assuming that n equals 6.9²³⁾, activation energies for high temperature (873K–1073K) deformation are about 251, 258, 316, and 323 KJ/mol at oxidation conditions of 1323 K–5, 10, 30 and 60 minutes in steam, respectively. Also activation energy of non-oxidized specimen heat-treated (1323 K–10min.) in a vacuum of 5×10^{-5} TORR is about 244 KJ/mol.

The fact that activation energies for plastic deformation of oxidized material are higher than that (~200 KJ/mol) of as-received one^{21,24,25,26)} may be due to the structural change and increase in ox-

xygen contents during oxidation, that is, further oxidation results in increase in activation energy. However since the mechanism for plastic deformation of the oxidized composite is very complex, it is difficult to clarify the reason clearly. Also very little work was performed with respect to activation energy of the oxidized composite.

4.4 Empirical Relation between Oxide Layer Thickness and Yield Stress

Since the objective of the present work is to obtain a correlation between oxide layer thickness and yield stress, an empirical relation can be derived as follows :

as in Eq.(25), $\sigma^n = \dot{\epsilon} / A \exp(Q/RT)$

The structure constant, A, should be dependent upon parameters related with structure of laminate. In present case, we are going to try the oxide layer thickness (expressed in ECR, %) as a parameter, so $\dot{\epsilon} / A$ can be replaced with CK^m .

where K : oxide layer thickness(ECR, %)

Thus, Eq.(25) can be expressed as follows,

$$\sigma^n = CK^m \exp(Q/RT) \dots\dots\dots (27)$$

By taking logarithms on both sides of Eq.(27)

$$\log \sigma = \frac{1}{n} \log [C \exp(Q/RT)] + \frac{m}{n} \log k \dots\dots\dots (28)$$

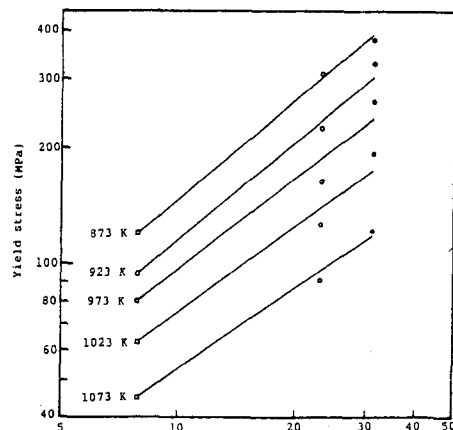


Fig.8 Variation of Yield Stress with Oxide Layer Thickness (expressed in ECR) at Various Temperatures

When relation in terms of $\log \sigma$ vs. $\log K$ is plotted to get the values of m and C as shown in Fig.8,

the slope ($\frac{m}{n}$) is obtained to be approximately 0.827, therefore $m=5.7$ ($n=6.9$) and the values of C are calculated as 2.6×10^{-6} , 1.15×10^{-6} , 1.19×10^{-9} , and 5.79×10^{-10} at oxidation conditions of 1323 K-5, 10, 30, and 60 minutes in steam, respectively.

Thus, empirical relation between ECR (K , %) and applied stress (σ) can be as follows,

$$\sigma^n = CK^m \exp(Q/RT) \quad [\text{or } (\frac{\sigma}{C})^n = K^m \exp(Q/RT)]$$

with

$$n=6.9$$

$$m=5.7$$

$$C=2.62 \times 10^{-6}, 1.15 \times 10^{-6}, 1.19 \times 10^{-9}, \text{ and } 5.79 \times 10^{-10} \text{ (or } 0.155, 0.138, 0.051, \text{ and } 0.046 \text{ MPa)}$$

for $Q=251, 258, 316, \text{ and } 323 \text{ KJ/mol}$, respectively

5. Conclusions

Expanding copper mandrel test is used to study the effect of oxidation on the yield stress and activation energy for high temperature plastic deformation of Zircaloy-4 cladding tube. The following conclusions are obtained;

- (1) Weight gain and oxide layer thickness during high temperature (1323 K) steam oxidation are linearly proportional to square root of time, that is,

$$K_i = \delta_{\text{kit}}^{1/2}$$

their proportional constant, δ_{ki} , are

$$0.281 \text{ for weight gain } [\text{mg} \cdot \text{cm}^2 \cdot \text{sec}^{-1/2}]$$

$$, 2.82 \text{ for thickness of ZrO}_2 \text{ layer } [\mu\text{m} \cdot \text{sec}^{-1/2}] \text{ and}$$

$$, 2.313 \text{ for thickness of } \alpha \text{ (O) layer } [\text{m} \cdot \text{sec}^{-1/2}]$$

- (2) The empirical relation between oxide layer

thickness (ECR, %) and yield stress can be expressed as,

$$(\frac{\sigma}{C})^n = K^m \exp(\frac{Q}{RT})$$

with

$$n=6.9, m=5.7,$$

$$C=0.155, 0.138, 0.051, \text{ and } 0.046 \text{ [MPa] for } Q=251, 258, 316, \text{ and } 323 \text{ KJ/mol, respectively.}$$

- (3) Activation energy for high temperature (873–1073 K) plastic deformation increases from 251 KJ/mol to 323 KJ/mol with increase in oxidation time from 5 minutes to 60 minutes.
- (4) Yield stress ($\sigma_{y0.2\%}$) of Zircaloy-4 increases with increase in oxidation time due to high strengthened ZrO₂.

References

1. F.J. Erbacher and S. Leistikow, "Zircaloy Fuel Cladding Behavior in a Loss of Coolant Accident: A Review", ASTM STP 939, (1987) 451-488
2. B.N. Mehrotra and K. Tangri, "High Temperature (600–800°C) Thermally Activated Deformation Behaviour of σ -Zircaloy-4 Oxygen Alloy", Acta Metal. 28(1980) 1385-1394
3. Rulemaking hearing, Acceptance Criteria for Emergency Core Cooling Systems for Light Water Cooled Nuclear Reactor, DOCKET RM-50-1, 1973
4. J.K. Yi and B.W. Lee, "Out-of Pile Test for Yielding Behavior of PWR Fuel Cladding Material", J. of Korean Nucl. Soc. 19(1987) 22-33
5. H.B. Park and B.W. Lee, "Expanding Copper Mandrel Test Evaluation of Yielding and Strain Aging Behavior of Zircaloy-4 PWR Fuel Clad Tube", MS Thesis, KAIST, 1987
6. R.E. Pawel, "Zirconium Metal-Water Oxidation Kinetics III. Oxygen Diffusion in Oxide and Alpha Zry Phases", ORNL/NUREG-53, 1976

7. B. Cox, *J. Electrochem. Soc.* 108(1961) 24–30
8. J.A. Davies, B. Donij, J.P.S. Pringle and F. Brown, *J. Electrochem. Soc.* 112(1965) 675–680
9. K.S. Rheem and W.K. Park, “Strain Ageing in Zircaloy-4”, *J. of Korean Nucl. Soc.* 8(1976) 19–27
10. K. Veevers, “Strain Ageing in Zirconium Alloys”, *J. of Nucl. Mat.* 55(1975) 109–110
11. W.D. Kingery, H.K. Bowen, and D.R. Uhlmann, “Introduction to Ceramics”, (1975) 603–774
12. G.E. Dieter, “Mechanical Metallurgy, 3rd ed.”, McGraw-hill, 1986
13. R.G. Reed-Hill, “Physical Metallurgy, 2nd ed.”, University Series in Basic Engineering, (1973) 346–353
14. L.J. Broutman, “Composite Materials”, 4(1974) 8–52
15. C. Kittel, “Introduction to Solid State Physics, 2nd ed.”, John Wiley and Son Inc., (1956) 152
16. D.L. Hagrman et al., “MATPRO-Version 11, A Handbook of Materials Properties for Use in the Analysis of LWR Fuel Rod Behavior”, EG&G, 1979
17. T. Nakajima et al., “FEMAXI-III, A Computer Code for the Analysis of Thermal and Mechanical Behavior of Fuel Rods”, JAERI-1298, 1985
18. L.R. Bunnell, “High Temperature Properties of Zircaloy-Oxygen Alloys”, EPRI/NP-524, 1977
19. Y.S. Touloukian, “Thermophysical Properties of High Temperature Solid Materials, Vol. 1 : Elements”, Purdue University, (1967) 462–463
20. D.L. Douglass, “The Metallurgy of Zirconium”, (1971) 41–76
21. A.T. Donaldson and H.E. Evans, “Oxidation-Induced Creep in Zircaloy-2”, *J. of Nucl. Mat.* 99(1981) 38–56
22. J.H. Brophy, P.M. Rose and J. Wulff, “The Structure and Properties of Materials V.II”, (1964) 63–67
23. C.E.L. Hunt, W.G. Newell, “Effect of β -phase Heat Treatment on the Subsequent α -Phase Ballooning Behavior of Zircaloy-4 Fuel Sheaths”, ASTM STP 681, (1979) 447–464
24. E.R. Gilbert, S.A. Duran and A. L. Bement, “Creep of Zirconium from 50 to 850°C”, ASTM STP 458, (1969) 210
25. V. Fidleris, “Uniaxial in-Rx. Creep of Zirconium Alloys”, *J. of Nucl. Mat.* 26(1968) 51–76
26. B. Burton, A.T. Donaldson and G.L. Reynolds, “Interaction of Oxidation and Creep in Zircaloy-2” ASTM STP 681, (1979) 561–585